Articles

Self-Assembly of Zinc Oxide Thin Films Modified with Tetrasulfonated Metallophthalocyanines by One-Step Electrodeposition

Tsukasa Yoshida,*,† Masashi Tochimoto,† Derck Schlettwein,‡ Dieter Wöhrle,§ Takashi Sugiura,† and Hideki Minoura†

Department of Chemistry, Faculty of Engineering, Gifu University, Yanagido 1-1, Gifu 501-1193, Japan, and Institut für Angewandte und Physikalische Chemie and Institut für Organische und Makromolekulare Chemie, Universität Bremen, NW 2, P.O. Box 330440, D-28334 Bremen, Germany

Received September 8, 1998. Revised Manuscript Received August 6, 1999

Cathodic electrodeposition in an aqueous mixed solution of zinc nitrate and water-soluble tetrasulfonated metallophthalocyanines (TSPcMs), in which M = Zn(II) (TSPcZn), Al(III)-[OH] (TSPcAl), or Si(IV)$[OH]_2$ (TSPcSi), resulted in a self-assembled growth of zinc oxide (ZnO) thin films whose surface is modified by TSPcMs. It has been found that the adsorption of TSPcM onto the growing surface of ZnO strongly affects the crystal growth and the orientation of the ZnO crystallites. The effect was most prominently seen with TSPcSi, creating a film looking like stacking disks aligned perpendicular to the substrate. Crystallographic studies by X-ray diffraction and TEM observation coupled with the selected area electron beam diffraction have revealed that thin platelike crystals, whose planes and edges correspond to the (002) and (100) crystal faces, respectively, are aligned in the same orientation around the *c*-axis within the stacks. The evolution of this unique structure is interpreted as arising from the preferential adsorption of TSPcMs at the (002) planes, leading to film growth preferentially in the (100) direction. Optical analysis of the films also revealed high order in the interactions among TSPcMs. Because of the strong intermolecular attraction, TSPcZn forms multilayers of π-stacking aggregates on ZnO as confirmed by the characteristic blueshift of the Q-band absorption. Thus, TSPcZn could be condensed at a very high concentration exceeding 1 M in the deposited film. These surface aggregates were completely removed by dipping the film in a solution of cationic detergent, cetyltrimethylammonium chloride, while only leaving surface-bound monomeric TSPcZn. By contrast, the aggregation was hindered for TSPcAl and TSPcSi because of the presence of axially coordinated OH^-, and monomeric adsorption was found in the electrodeposited films.

Introduction

Thin film processing of inorganic and organic materials is a key technology in device fabrication. Because the function exhibited from a device using such materials is a sum of the phenomena occurring at the molecular, ionic, and atomic levels, precise control of chemical and physical structure of the film upon processing should result in a drastic improvement of the device performance. However, the technology must also be developed in view of economy and ecology. Although gas-phase techniques such as vacuum evaporation, sputtering, chemical vapor deposition, or molecular beam epitaxy have successfully achieved ordered growth of inorganic compound thin films[1,2] or thin films of organic molecules,[3,4] these techniques inevitably need high temperature or vacuum, making them disadvantageous for large-scale productions. Film processing employing chemical and electrochemical reactions in solutions bears the highest advantages in this respect. Because the starting materials are in solvated forms, the huge energy needed to produce gaseous atoms, ions or molecules in the gas-phase techniques can be saved.[5] The use of solutions also facilitates the collection and recycling of the waste materials.

† Gifu University.
‡ Institut für Angewandte und Physikalische Chemie.
§ Institut für Organische und Makromolekulare Chemie.

(1) Tong, W.; Wagner, B. K.; Tran, T. K.; Ogle, W.; Park, W.; Summers, C. J. *J. Cryst. Growth* **1996**, *164*, 202.
(2) Kang, H.-B.; Nakamura, K.; Lim, S.-H.; Shindo, D. *Jpn. J. Appl. Phys.* **1998**, *37*, 781.
(3) Morioka, T.; Tada, H.; Koma, A. *J. Appl. Phys.* **1993**, *73*, 2207.
(4) Schmidt, A.; Schlaf, R.; Louder, D.; Chau, L.-K.; Chen, S.-Y.; Fritz, T.; Lawrence, M. F.; Parkinson, B. A.; Armstrong, N. R. *Chem. Mater.* **1995**, *7*, 2127.
(5) Yoshimura, M.; Suchanek, W. *Solid State Ionics* **1997**, *98*, 197.

10.1021/cm980619o CCC: $18.00
Published on Web 09/30/1999

Although ordered growth of inorganic compound thin films has been successfully achieved by chemical[6−9] and electrochemical[8−12] methods, very few examples can be found for the electrodeposition of organic molecules such as phthalocyanines.[13,14] Saji and Ishii have realized electrodeposition of solid phthalocyanine thin films from water by using electrooxidative disruption of micelles composed of surfactant molecules having redox-active ferrocenyl groups, although precise control of the film structure seems to be difficult with this technique because phthalocyanines are present as clusters in solution and the film growth takes place by randomly piling them up on the substrate.[13] Thin films of phthalocyanines have been also prepared together with other substances, such as those embedded in Langmuir−Blodgett films,[15] mixed with or covalently bound to polymers,[16−18] dispersed in inorganic thin film by mixing during its sol−gel processing[19] or spray pyrolysis,[20] and chemically adsorbed onto inorganic surfaces from solutions.[21−23] The use of supporting materials not only facilitates the film formation but also can enhance the functions of the organic molecules or can add new properties, for example, in catalysis,[17] chemical sensing,[24,25] photochromism,[26] electroluminescence,[27] lasing,[28] nonlinear optics[29] and photoenergy conversion.[20−22,30,31] One of the most successful applications of such materials can be found in the recent progress of dye-sensitized solar cells, in which photoactive organic dyes and inorganic semiconductors cooperate in the photoinduced charge separation process.[30,31] Phthalocyanines are promising candidates as sensitizers owing to their high visible light absorption and high chemical stability.[20−22]

Preparation of the dye-modified inorganic semiconductor thin films has been done by stepwise processing in most of the previous studies, namely, sol−gel processing of porous inorganic semiconductor thin films, followed by dye adsorption from solutions.[21−22,30,31] We have recently found that cathodic electrodeposition from an aqueous solution containing zinc nitrate and water-soluble organic dyes having sulfonic acid groups such as 2,9,16,23-tetrasulfophthalocyaninatozinc(II) (TSPc-Zn) or tetrabromophenol blue (TB) results in a one-step formation of zinc oxide (ZnO) thin films whose surface is modified by these dyes.[32,33] The deposited dye-modified ZnO thin films have been found to perform as sensitized photoelectrodes, thus opening up a new synthetic route to the photoactive materials in dye-sensitized solar cells.[33,34] The presence of the dye molecules in the deposition bath not only realized their loading into ZnO but also was found to affect the growth of ZnO. Whereas the film deposited in a pure $Zn(NO_3)_2$ aqueous solution was made of densely packed, well-crystallized ZnO particles, the adsorption of the added dye molecules during the film deposition hindered the crystal growth of ZnO to produce a porous film.[32] It has been also found that the dye molecules are not just passively "included" during the ZnO growth but actively participate in the electrode process, as observed in the enhancement of the electroreduction of TB by Zn^{2+} and concomitant attenuation of the reduction of NO_3^- in the TB+$Zn(NO_3)_2$ mixed solution.[33] Anchoring of the dye molecules through their sulfonic acid groups was evidenced for the electrodeposited ZnO/TB thin film, in which a pH-sensitive color change of TB that is usually seen for the TB molecules having free sulfonate was completely prohibited.[33]

The self-assembly of these mixed materials is governed not only by the chemical interaction between the ZnO surface and the dye molecules but also by that among the adsorbed molecules. Formation of ordered dye aggregates was evidently seen in both the ZnO/TSPcZn and ZnO/TB thin films.[32,33] Ordered assemblies of organic molecules on inorganic surfaces, typically thiols on gold, have actively been studied in recent years and are frequently called self-assembled monolayers (SAMs).[25,35−37] The evolution of SAMs is made possible not only by the coordination of −SH groups to the ordered gold surface but also by the chemical interactions within the neighboring molecules.[35−37] The main

(6) Froment, M.; Bernard, M. C.; Cortes, R.; Mokili, B.; Lincot, D. *J. Electrochem. Soc.* **1995**, *142*, 2642.
(7) Nicolau, Y. F.; Dupuy, M.; Brunel, M. *J. Electrochem. Soc.* **1990**, *137*, 2915.
(8) Gorer, S.; Ganske, J. A.; Hemminger, J. C.; Penner, R. M. *J. Am. Chem. Soc.* **1998**, *120*, 9584.
(9) Yamaguchi, K.; Yoshida, T.; Sugiura, T.; Minoura, H. *J. Phys. Chem. B* **1998**, *102*, 9677.
(10) Golan, Y.; Hodes, G.; Rubinstein, I. *J. Phys. Chem.* **1996**, *100*, 2220.
(11) Huang, B. M.; Colletti, L. P.; Gregory, B. W.; Anderson, J. L.; Stickney, J. L. *J. Electrochem. Soc.* **1995**, *142*, 3007.
(12) Hayden, B. E.; Nandhakumar, I. S. *J. Phys. Chem. B* **1998**, *102*, 4897.
(13) Saji, T.; Ishii, Y. *J. Electrochem. Soc.* **1989**, *136*, 2953.
(14) Fukuzawa, T.; Koyama, T.; Schneider, G.; Hanabusa, K.; Shirai, H. *J. Inorg. Organomet. Polym.* **1994**, *4*, 261.
(15) Osburn, E. J.; Chau, L.-K.; Shen, S.-Y.; Collins, N.; O'Brien, D. F.; Armstrong, N. R. *Langmuir* **1996**, *12*, 4784.
(16) Schlettwein, D.; Kaneko, M.; Yamada, A.; Wöhrle, D.; Jaeger, N. I. *J. Phys. Chem.* **1991**, *95*, 1748.
(17) Yoshida, T.; Kamato, K.; Tsukamoto, M.; Iida, T.; Schlettwein, D.; Wöhrle, D.; Kaneko, M. *J. Electroanal. Chem.* **1995**, *385*, 209.
(18) Wöhrle, D. In *Phthalocyanines, Properties and Applications*; Leznoff, C. C., Lever, A. B. P., Eds.; VCH: New York, 1989; Vol. 1, pp 55−132.
(19) Schubert, U.; Lorenz, A.; Kundo, N.; Stuchinskaya, T.; Gogina, L.; Salanov, A.; Zaikovskii, V.; Maizlish, V.; Shaposhnikov, G. P. *Chem. Ber./Recl.* **1997**, *130*, 1585.
(20) Yanagi, H.; Ohoka, Y.; Hishiki, T.; Ajito, K.; Fujishima, A. *Appl. Surf. Sci.* **1997**, *113/114*, 426.
(21) Deng, H.; Mao, H.; Zhang, H.; Lu, Z.; Xu, H. *J. Porphyrins Phthalocyanines* **1998**, *2*, 171.
(22) Nazeeruddin, M. K.; Humphry-Baker, R.; Grätzel, M.; Wöhrle, D.; Schnurpfeil, G.; Schneider, G.; Hirth, A.; Trombach, N. *J. Porphyrins Phthalocyanines* **1999**, *3*, 230.
(23) Schlettwein, D.; Yoshida, T. *J. Electroanal. Chem.* **1998**, *441*, 139.
(24) Moore, D. E.; Lisensky, G. C.; Ellis, A. B. *J. Am. Chem. Soc.* **1994**, *116*, 9487.
(25) Taniguchi, I. *Electrochem. Soc. Interface* **1997**, *6*, 34.
(26) Bonhôte, P.; Moser, J. E.; Vlachopoulos, N.; Walder, L.; Zakeeruddin, S. M.; Humphry-Baker, R.; Péchy, P.; Grätzel, M. *Chem. Commun.* **1996**, 1163.
(27) Athanassov, Y.; Rotzinger, F. P.; Péchy, P.; Grätzel, M. *J. Phys. Chem. B* **1997**, *101*, 2558.
(28) Yanagi, H.; Hishiki, T.; Tobitani, T.; Otomo, A.; Mashiko, S. *Chem. Phys. Lett.* **1998**, *292*, 332.
(29) Roscoe, S. B.; Yitzchaik, S.; Kakkar, A. K.; Marks, T. J.; Xu, Z.; Zhang, T.; Lin, W.; Wong, G. K. *Langmuir* **1996**, *12*, 5338.
(30) O'Regan, B.; Grätzel, M. *Nature* **1991**, *353*, 737.
(31) Redmond, G.; Fitzmaurice, D.; Grätzel, M. *Chem. Mater.* **1994**, *6*, 686.
(32) Yoshida, T.; Miyamoto, K.; Hibi, N.; Sugiura, T.; Minoura, H.; Schlettwein, D.; Oekermann, T.; Schneider, G.; Wöhrle, D. *Chem. Lett.* **1998**, 599.
(33) Yoshida, T.; Yoshimura, J.; Matsui, M.; Sugiura, T.; Minoura, H. *Trans. MRS-J*, in press.
(34) Schlettwein, D.; Oekermann, T.; Yoshida, T.; Tochimoto, M.; Minoura, H. *J. Electroanal. Chem.*, submitted for publication.
(35) Yamada, R.; Uosaki, K. *Langmuir* **1998**, *14*, 855.
(36) Knoll, W.; Pirwitz, G.; Tamada, K.; Offenhäusser, A.; Hara, M. *J. Electroanal. Chem.* **1997**, *438*, 199.
(37) Wang, R.; Iyoda, T.; Jiang, L.; Tryk, D. A.; Hashimoto, K.; Fujishima, A. *J. Electroanal. Chem.* **1997**, *438*, 213.

difference in our one-step electrodeposition process is the fact that the inorganic surface is not preexisting, but is also self-assembled in a circumstance where the adsorption of organic molecules is in force.

In the present work, we have studied the one-step electrodeposition of ZnO in the presence of tetrasulfonated metallophthalocyanines (TSPcMs), in which M refers to Zn(II) (TSPcZn), Al(III)[OH] (TSPcAl) or Si(IV)$[OH]_2$ (TSPcSi). Although the phthalocyanine moiety is unchanged, the central metals of trivalent Al^{3+} and tetravalent Si^{4+} need to be charge-compensated by axial coordination of anions such as OH^-, hence making their π-stacking aggregation behavior very different from that of TSPcZn, which has no axial ligands.[38,39] The difference in the intermolecular chemical affinity of these molecules is expected to result in different self-assemblies. Detailed analyses of the products have been carried out on their structural, crystallographic, and optical properties, to elucidate the chemical nature of these unique materials.

Experimental Section

The sodium salts of 2,9,16,23-tetrasulfophthalocyaninatozinc(II) (TSPcZn), 2,9,16,23-tetrasulfophthalocyaninatohydroxoaluminum(III) (TSPcAl), and 2,9,16,23-tetrasulfophthalocyaninato-dihydroxosilicon(IV) (TSPcSi) were synthesized according to the procedure described in the literature.[39−41] All other chemicals used were of analytical reagent grade and were used without further purification. Doubly distilled and ion-exchanged water was used throughout the experiments. An indium tin oxide (ITO, 10 Ω/cm^2, Musashino Fine Glass) coated glass substrate was ultrasonically sequentially cleaned in acetone, 2-propanol, and water each for 15 min, prior to the film deposition.

The electrodeposition of ZnO was carried out potentiostatically at −0.7 or −0.9 V (vs SCE) for 60 min in a 0.1 M $Zn(NO_3)_2$ aqueous solution maintained at 70 °C.[42] The deposition of ZnO/TSPcM films was achieved simply by adding ca. 50 μM TSPcMs to the zinc nitrate bath. The deposited films were rinsed by water, dried in air at room temperature, and subjected to further analyses. Several kinds of ZnO+TSPcM mixed materials were prepared for comparison. A physical mixture of ZnO+TSPcM was prepared by mixing dry powders of ZnO (99.9%, Rare Metallics) and each of TSPcMs in a mortar. ZnO powder samples were also refluxed in aqueous solutions of each ca. 50 μM TSPcM for 1 h to promote chemical adsorption of TSPcM on their surface. The powders were filtered, washed by water, and dried in air. To study the surface aggregation of TSPcZn in more detail, the electrodeposited ZnO/TSPcZn thin film as well as the samples with adsorbed TSPcZn were treated in an aqueous solution of cationic detergent, 0.1 M cetyltrimethylammonium chloride (CTAC), which is known to break up the π-stacking aggregates and to assist in dissolution of TSPcZn in its monomeric form in water.[39]

X-ray diffraction patterns (XRD) of the deposited films were measured by a Rigaku RAD-2R using Cu Kα radiation. Surface morphologies of the films were observed by a Topcon ABT-150FS scanning electron microscope (SEM). Transmission electron micrographs (TEM) and complementary selected area electron diffraction (SAED) patterns of the deposits were obtained on a Hitachi H-8100 transmission electron microscope. Film thickness was determined by using a Kosaka SE−2300 surface profilometer. The UV−vis absorption spectra of the films and solutions were measured in transmission on a Hitachi U-3500 spectrophotometer. The visible absorption spectra of the powder samples were obtained by measuring the diffuse reflection spectra on a Hitachi U-4000 spectrophotometer and converting them by using the Kubelka−Munk function. The amount of TSPcM loaded into the film was determined by dissolving a known area of the deposited film into a known volume of concentrated (7 M) ammonia and measuring its absorption spectrum. In the case of TSPcZn, ca. 0.1 M CTAC was further added to the solution. Molar extinction coefficients (ϵ) of TSPcZn, TSPcAl, and TSPcSi are 155 800, 132 000, and 91 100 M^{-1} cm^{-1}, respectively.[41]

Results and Discussion

Electrodeposition of ZnO. The SEM photograph of the ZnO thin film electrodeposited at −0.9 V in a pure $Zn(NO_3)_2$ aqueous solution is shown in Figure 1a. Faceted growth of hexagonal cylindrical particles of 0.4−0.7 μm in diameter is seen. A thickness of 0.96 μm is reached for this film, showing that only a few particles can be present along the depth of the film. The film growth in the present system therefore is achieved by growth of ZnO crystallites and not by piling up particles of ZnO. The electrochemical reduction of nitrate has been frequently used in the electrodeposition of metal oxides[41,43−45] or hydroxides.[46,47] We have confirmed that nitrate is reduced to nitrite and partly to ammonia along with the cathodic electrodeposition of ZnO, by analyzing the zinc nitrate solution after the electrolysis by ion chromatography. The reduction of nitrate was not observed in an aqueous solution of KNO_3 upon electrolysis carried out under the same conditions.

It has been reported that the reduction of nitrate takes place in the presence of certain metal cations which are expected to get adsorbed on the electrode surface.[48] The potential for the reduction of nitrate was found to shift positively in accordance with the positive shift of the reduction potentials of the coexisting metal cations to their corresponding metals.[49] The potential changes also with respect to the variation of the equilibrium constants for the first hydrolysis of the metal ions ($M^{n+} + H_2O \rightarrow [M(OH)]^{(n-1)+} + H^+$).[50] The reduction of nitrate generates OH^-, which is subsequently captured by the metal ion to produce its hydroxides or oxides upon dehydration. Therefore, the metals having high stability constants for its hydroxide species would favor the reduction of nitrate. With the above-mentioned discussion in mind, the electrodeposition of ZnO in the present system is expected to proceed as follows. The Zn^{2+} ion mediates the charge transfer for the electroreduction of nitrate to nitrite and ammonia as in eqs 1 and 2, respectively.

(38) Yoon, M.; Cheon, Y.; Kim, D. *Photochem. Photobiol.* **1993**, *58*, 31.
(39) Schneider, G.; Wöhrle, D.; Spiller, W.; Stark, J.; Schulz-Ekloff, G. *Photochem. Photobiol.* **1994**, *60*, 333.
(40) Ali, H.; Langlois, R.; Wagner, J. R.; Brasseur, N.; Paquette, B.; van Lier, J. E. *Photochem. Photobiol.* **1988**, *47*, 713.
(41) Schneider, G. Ph.D. Thesis, University of Bremen, Bremen, Germany, 1995.
(42) Izaki, M.; Omi, T. *Appl. Phys. Lett.* **1996**, *68*, 2439.
(43) Natarajan, C.; Nogami, G. *J. Electrochem. Soc.* **1996**, *143*, 1547.
(44) Zhitomirsky, I.; Gal-Or, L.; Kohn, A.; Hennicke, H. W. *J. Mater. Sci.* **1995**, *30*, 5307.
(45) Zhou, Y.; Phillips, R. J.; Switzer, J. A. *J. Am. Ceram. Soc.* **1995**, *78*, 981.
(46) Matsumoto, Y.; Adachi, H.; Hombo, J. *J. Am. Ceram. Soc.* **1993**, *76*, 769.
(47) Streinz, C. C.; Hartman, A. P.; Motupally, S.; Weidner, J. W. *J. Electrochem. Soc.* **1995**, *142*, 1084.
(48) Cox, J. A.; Brajter, A. *Electrochim. Acta* **1979**, *24*, 517.
(49) Ogawa, N.; Kodaiku, H.; Ikeda, S. *J. Electroanal. Chem.* **1986**, *208*, 117.
(50) Ogawa, N.; Ikeda, S. *Anal. Sci. Suppl.* **1991**, *7*, 1681.

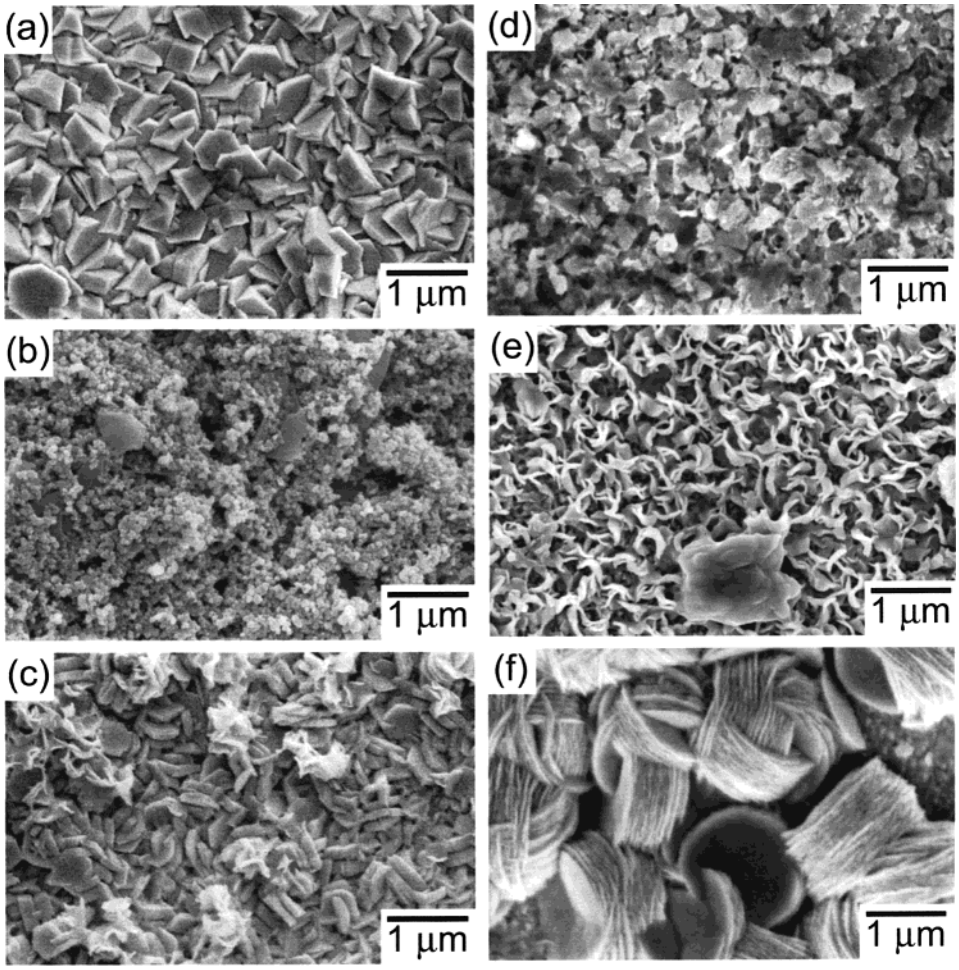

Figure 1. SEM photographs of a ZnO thin film electrodeposited at −0.9 V (a), ZnO/TSPcZn thin films electrodeposited at −0.7 (b) and −0.9 V (c), ZnO/TSPcAl thin films electrodeposited at −0.7 (d) and −0.9 V (e), and a ZnO/TSPcSi thin film electrodeposited at −0.9 V (f).

$$NO_3^- + H_2O + 2e^- \rightarrow NO_2^- + 2OH^- \quad (E° = -0.240 \text{ V vs SCE}) \quad (1)$$

$$NO_3^- + 6H_2O + 8e^- \rightarrow NH_3 + 9OH^- \quad (E° = -0.373 \text{ V vs SCE}) \quad (2)$$

The $E°$ values were calculated from the standard reaction Gibbs energies (ΔG) derived from the Gibbs free energy of formation at 298 K (ΔG_f) of each chemical species in aqueous phase obtained from literature.[51] The generated OH^- instantaneously reacts with Zn^{2+} ion to give zinc hydroxide, which, however, is dehydrated to produce the more stable zinc oxide.

$$Zn^{2+} + 2OH^- \rightarrow Zn(OH)_2 \rightarrow ZnO + H_2O \quad (3)$$

The actual reaction may not be stepwise as written above but is more likely to take place in one step because the same Zn^{2+} ion would play two roles: as the catalysis in the reduction of nitrate and as the precipitation (ZnO) that consumes the electrogenerated base. Consequently, the reaction may be better expressed by the overall reactions in eqs 4 and 5.

$$Zn^{2+} + NO_3^- + 2e^- \rightarrow ZnO + NO_2- \quad (E° = +0.246 \text{ V vs SCE}) \quad (4)$$

$$5Zn^{2+} + NO_3^- + 2H_2O + 8e^- \rightarrow 5ZnO + NH_4^+ \quad (E° = +0.213 \text{ V vs SCE}) \quad (5)$$

It is important to note that these electrochemical reactions are expected to take place at the ZnO/electrolyte interface, as evident from the observed crystal growth, which can only be achieved by surface reactions. It is therefore expected that addition of adsorbates to such a system affects the crystal growth, thus resulting in different film morphologies.

Morphology of the Electrodeposited ZnO/TSPcM Films. The addition of TSPcZn, TSPcAl, and TSPcSi indeed resulted in very different morphologies of the films as shown in Figure 1. The morphology was also changed by the deposition potentials. All of the films deposited in the presence of TSPcMs are blue or blue-green, although the degree of coloration varied very much depending on both the kind of the TSPcM molecules and the deposition potentials used. The film thickness, the amount of TSPcM loaded into the porous film, and the concentration of TSPcM in the film (assuming its homogeneous distribution in the film) are listed in Table 1. No film was deposited when the electrolysis was performed at −0.7 V and in the presence of TSPcSi. It is noticed that the addition of TSPcM

(51) Dean, J. A. *Lange's Handbook of Chemistry*, 14th ed.; McGraw-Hill: New York, 1992; Section 6 .

Table 1. Film Thickness, Amount of Loaded TSPcM, and Concentration of TSPcM in the Films, Determined for the Electrodeposited ZnO/TSPcZn, ZnO/TSPcAl and ZnO/TSPcSi Thin Films

films	deposition potential (V vs SCE)	film thickness (nm)	amount of TSPcM loaded ($nmol/cm^2$)	TSPcM concn in the film[a] ($mmol/cm^3$)
ZnO	−0.9	960		
ZnO/TSPcZn	−0.7	500	58.3	1.16
	−0.9	1600	5.39	0.0337
ZnO/TSPcAl	−0.7	730	13.0	0.178
	−0.9	1120	8.90	0.0793
ZnO/TSPcSi	−0.9	1180	1.41	0.0119

[a] Concentration assuming homogeneous distribution of TSPcM in the porous films.

increases the film thickness determined by a surface profilometer, because of the increased porosity of the TSPcM-modified ZnO films.

The ZnO/TSPcZn film deposited at −0.7 V was highly transparent and intense blue, as noticed from the very large amount of the TSPcZn loaded into the film. The concentration of TSPcZn in this film is as high as 1.16 $mmol/cm^3$, which is almost 10 times higher than the concentration of the Ru−polypyridine complexes in the colloid-processed TiO_2 films (0.13 $mmol/cm^3$) successfully applied to dye-sensitized solar cells.[30] The cause of this high concentration of TSPcZn in the film will be discussed later in this paper. A clear change of the film morphology is observed. As seen in Figure 1b, the film is highly porous, consisting of very fine particles of 20−50 nm in diameter and a few platelike large particles. The small particle size is expected to reduce light scattering and hence increase the transparency of the film. The crystallinity of ZnO became much lower than that of the pure ZnO as found in the XRD analysis of the film.[32] The adsorption of TSPcZn onto the growing surface of ZnO is supposed to hinder further crystal growth of ZnO, thus creating a film of very fine particles.

The deposition of the ZnO/TSPcZn film at −0.9 V decreased the dye loading by one-tenth, despite a film thickness three times higher than that deposited at −0.7 V (Table 1). The SEM photograph of this film (Figure 1c) shows that the particle size is considerably larger, indicating the higher crystallinity of ZnO in the film. It is supposed that the increased cathodic overvoltage accelerated the rate of the ZnO crystal growth relative to that of the dye adsorption, thus resulting in the larger film thickness and better crystallinity of ZnO but a lower concentration of TSPcZn, compared to that of the film deposited at −0.7 V. A careful look at the picture reveals that the particles again have a hexagonal shape, although somewhat flatter than that of pure ZnO. These particles are largely aligned with their hexagonal planes perpendicular to the substrate, as recognized from the exposed rectangular edges of the particles The preferential orientation of the ZnO crystallites will be analyzed further in the crystallographic studies performed on these films (vide infra).

The ZnO/TSPcAl films are also porous; however, they consist of particles with indistinctive shape (Figure 1d,e). When the film deposition was carried out at −0.7 V, TSPcAl was loaded to the film in a much smaller amount than TSPcZn under the same conditions, although the highest dye concentration was achieved for TSPcAl among the three when the deposition was carried out at −0.9 V.

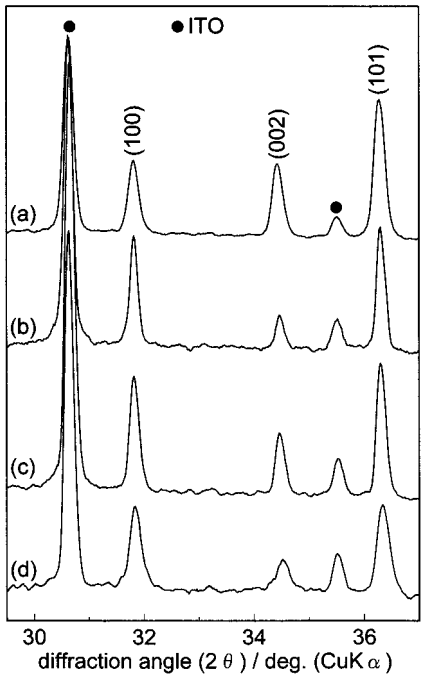

Figure 2. X-ray diffraction patterns for the thin films of ZnO (a), ZnO/TSPcZn (b), ZnO/TSPcAl (c) and ZnO/TSPcSi (d) electrodeposited at −0.9 V.

The ZnO/TSPcSi film has a very unique morphology (Figure 1f). The films consist of stacks of disklike particles, which are as large as 1.5 μm in diameter and as thin as several tens of nanometers in thickness. Although some irregularities are seen, most of the disk stacks are arranged with their disk planes perpendicular to the substrate. It should be noted that the dye loading was the least efficient with TSPcSi (Table 1), yet it caused a drastic change of the film morphology. These unique disk stacks certainly deserve to be analyzed in more detail to discuss their crystallographic properties. It should also be noted that the concentration of the TSPcM molecules in the deposition bath is very much lower than that of $Zn(NO_3)_2$ for more than 3 orders of magnitude. A slight change of surface conditions caused by the adsorption of TSPcM molecules is sufficient to cause the observed significant changes in the ZnO crystal growth.

Crystallographic Analysis and Growth Mechanism of the ZnO/TSPcM Films. XRD spectra were measured for ZnO, ZnO/TSPcZn, ZnO/TSPcAl, and ZnO/TSPcSi thin films electrodeposited at −0.9 V. All films showed sharp diffraction peaks assigned to ZnO, aside from the peaks arising from the ITO substrate. In Figure 2 are shown the diffraction patterns for the three major peaks arising from the (100), (002), and (101) planes of the hexagonal structure. It is noticed that the relative peak intensities for the ZnO/TSPcM films are different from those of the pure ZnO, indicating differences in their crystallographic orientation. While the peak intensity from the (002) planes decreases, the (100) peak becomes larger for the films deposited with TSPcMs.

To analyze the change of the crystal orientation more quantitatively, orientation indices were calculated for each XRD pattern (Table 2) using the following strategy. An intensity factor (IF_{hkl}) is defined as the ratio of the peak intensity for the diffraction peak of interest,

Table 2. Intensities of the Diffraction Peaks ($I_{(hkl)}$), Intensity Factors ($IF_{(hkl)} = I_{(hkl)}/\Sigma I_{(hkl)}$) and Orientation Indices Relative to the Standard Powder Sample ($OIS_{(hkl)} = IF_{(hkl)}/IFS_{(hkl)}$) and Relative to the ZnO Thin Film Electrodeposited without TSPcM ($OIZ_{(hkl)} = IF_{(hkl)}/IFZ_{(hkl)}$) As Determined from the XRD Spectra in Figure 2

sample	*hkl*	$I_{(hkl)}$	$IF_{(hkl)}$	$OIS_{(hkl)}$	$OIZ_{(hkl)}$
ZnO powder std[a]	100	57	0.284 ($IFS_{(100)}$)		
	002	44	0.219 ($IFS_{(002)}$)		
	101	100	0.498 ($IFS_{(101)}$)		
ZnO thin film	100	279	0.244 ($IFZ_{(100)}$)	0.859	
	002	297	0.259 ($IFZ_{(002)}$)	1.182	
	101	569	0.497 ($IFZ_{(101)}$)	0.998	
ZnO/TSPcZn thin film	100	376	0.397	1.398	1.627
	002	114	0.120	0.548	0.463
	101	458	0.483	0.970	0.970
ZnO/TSPcAl thin film	100	452	0.363	1.278	1.488
	002	244	0.196	0.895	0.757
	101	550	0.441	0.886	0.887
ZnO/TSPcSi thin film	100	211	0.396	1.394	1.623
	002	79	0.149	0.680	0.575
	101	242	0.455	0.914	0.915

[a] Data from Joint Committee on Powder Diffraction Standards (JCPDS), Card 36-1451.

relative to the sum of the intensities of the diffraction peaks in question, thus for these three peaks is expressed, for example, as follows:

$$IF_{(100)} = \frac{I_{(100)}}{I_{(100)} + I_{(002)} + I_{(101)}} \quad (6)$$

where $I_{(hkl)}$ refers to the diffraction peak intensity in XRD. The standard intensity factors, $IFS_{(hkl)}$, were obtained from the data of a standard powder sample (JCPDS). The intensity factors of the pure ZnO thin film electrodeposited without TSPcMs were also considered as standards ($IFZ_{(hkl)}$) because they give better estimates for the effect of the addition of TSPcMs to change the crystal orientations of the electrodeposited films. The orientation indices are then determined by dividing the $IF_{(hkl)}$'s of the diffraction peak of interest by the standard intensity factors, for example, in the case of the (100) diffraction peak as

$$OIS_{(100)} = \frac{IF_{(100)}}{IFS_{(100)}} \quad (7)$$

referred to the powder sample or

$$OIZ_{(100)} = \frac{IF_{(100)}}{IFZ_{(100)}} \quad (8)$$

referred to the electrodeposited ZnO. Any crystal planes for which these values exceed 1 are preferentially oriented parallel to the substrate, whereas those with the orientation indices less than 1 have the tendency not to be parallel to the substrate.

It is noticed that the ZnO thin film deposited without TSPcMs is somewhat oriented with its (002) planes parallel to the substrate as indicated from its $OIS_{(002)}$ value being larger than 1. Consistently, the $OIS_{(100)}$ becomes less than 1. Examination of $OIS_{(hkl)}$ for the ZnO/TSPcM thin films reveals just the opposite in the crystal orientation, showing the highest values for their $OIS_{(100)}$. For the ZnO/TSPcZn and ZnO/TSPcSi thin films, the $OIS_{(002)}$ value becomes significantly smaller than 1, whereas $OIS_{(101)}$ does not change very much. This clearly indicates that the *c*-axes of the ZnO crystallites are turned by 90° from the (002) preferential orientation parallel with the substrate to the (100) preference, by adding TSPcZn or TSPcSi to the deposition bath. In the case of TSPcAl, the $OIS_{(100)}$ also gets larger than 1 at the expense of $OIS_{(002)}$ with, however, $OIS_{(101)}$ decreasing almost equally, suggesting that the change of the crystal orientation is not as simple as in the case of TSPcZn and TSPcSi. Such difference in the crystal growth may be attributable to the asymmetric molecular structure of TSPcAl relative to the Pc plane, because it has only one axial ligand, whereas TSPcZn and TSPcSi are symmetric. It is, however, safe to conclude that the addition of TSPcM into the deposition bath alters the crystal orientation from the (002) parallel with substrate preference to (100) parallel with substrate preference, as found from the $OIZ_{(hkl)}$ values for which all of TSPcMs enhances $OIZ_{(100)}$ while decreasing $OIZ_{(002)}$. The (100) parallel with substrate crystallographic orientation found in the XRD analysis is directly related to abovementioned analysis that the disklike deposits are standing on the substrate with their edge found in the SEM observation of the ZnO/TSPcZn and ZnO/TSPcSi films. The edge of these disks corresponds to the (100) crystal face of ZnO, whereas the disk plane corresponds to (002).

The crystal structure of the stacking disks has been studied in more detail by TEM, after the ZnO/TSPcSi thin film was scratched off the ITO substrate. Several large deposits were found, which would correspond to the disk stacks. They were as large as 2 μm in diameter, are shown in the lower part of Figure 3A, and did not allow the electron beam to penetrate. Fortunately, there were several thin and flat particles that allowed the penetration of the electron beam, as shown in the upper part of Figure 3A. It supposedly is of "a few" disks that together were thin enough for the TEM observation. In the high-magnification image of the thinner deposit, a uniform lattice image was found with ca. 2.8 Å interspace over the entire deposit, as shown in the lower inset of Figure 3A. This corresponds to the lattice fringe created by lateral projection of (100) planes of ZnO. The complementary SAED diffraction pattern is shown as the upper inset of Figure 3A, and it clearly exhibits diffraction spots in a 6-fold symmetry. They could be indexed by taking the [001] zone axis as shown in the figure. The SAED pattern with clear spots indicates perfect orientation of the disks around their *c*-axes within the stack.

Images vertical to the disk edges are shown in Figure 3B. It can be seen that the disk stack consists of fine particles connected and aligned in the same direction, although the deposit shown in Figure 3B might have been destroyed mechanically, because a large part of it allows penetration of the electron beam. The perfect disk stacks should be too large to allow any TEM observation. The high-magnification image of the deposit (the lower inset of Figure 3B) still exhibited several lattice images of crystals that are aligned in almost the same direction as that of the disklike deposits and have a lattice constant of ca. 2.6 Å, which corresponds to the lattice fringe produced by the (002) planes. The deposits were too small to obtain their exact SAED pattern. The

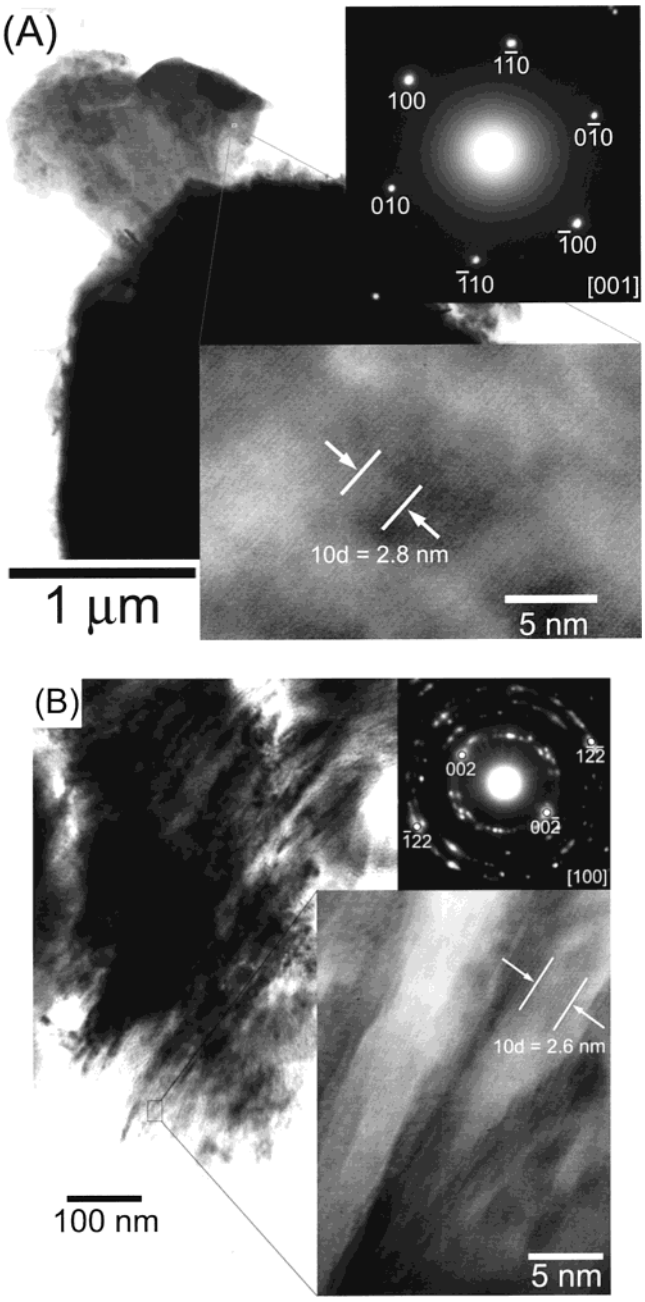

Figure 3. TEM images of the "disks" consisting of the ZnO/TSPcSi thin film seen in Figure 1f. (A) View vertical to the disk plane together with the high magnification image showing the lattice fringe with ca. 2.8 Å interspace corresponding to the (100) planes of ZnO and the complementary SAED pattern showing 6-fold diffraction spots indexed by taking [001] zone axis. (B) View vertical to the edge of the stacking disks together with the high magnification image showing the lattice fringe with ca. 2.6 Å interspace corresponding to the (002) planes of ZnO and the complementary SAED pattern in which several bright spots are indexed by taking [100] zone axis.

diffraction pattern showing many spots was only obtained as shown in the upper inset of Figure 3B, reflecting certain irregularities of the crystal orientations within the observed area. However, the brightest spots in the diffraction pattern could be indexed by taking the [100] zone axis, thus confirming that the disk stack is observed from its edge in the TEM image of Figure 3B. These TEM images and SAED patterns confirm that the disk planes and edges correspond to the (002) and (100) crystal faces of ZnO, respectively, and the disks are aligned in a high order relative to the *c*-axis within the stack.

With the above findings about the crystallographic structure of the ZnO/TSPcM thin films in mind, a growth mechanism is proposed as illustrated in Figure 4. Although a slightly different crystallographic orientation has been found for ZnO/TSPcAl, this model should be valid to explain the growth of the films in the observed structures, especially for ZnO/TSPcZn and ZnO/TSPcSi. The anchoring of TSPcM to ZnO is expected to occur through the coordination of the sulfonic acid group to the surface Zn^{2+} ion of ZnO. Formation of the Ti−OSO_2−Pc bond was found by the FTIR analysis of sol−gel processed TiO_2/TSPcCo composite.[19] Such esterlike linkage between the dye molecule and the TiO_2 surface has also been found between carboxylic acid groups in dithiocyanato-*N*,*N*′-bis(2,2′-bipyridyl-4,4′-dicarboxylic acid) ruthenium(II) complex and surface OH^- of TiO_2,[52,53] which have been reported as the best combination for the dye-sensitized solar cells.[54] Our recent study on the electrodeposition of ZnO modified with TB from $Zn(NO_3)_2$+TB mixed solutions also revealed chemical bond formation between the sulfonic acid group of TB and the ZnO surface, which prohibited the pH-dependent color change of TB that is accompanied by a structural change of TB involving the $-SO_3^-$ group.[33] The adsorption of TSPcM is then expected to occur preferentially onto the (002) crystal faces of ZnO to hinder the crystal growth along the *c*-axis. The growth of ZnO crystallites, thus film growth, therefore tends to occur in the (100) direction. The observed alignment of the ZnO crystals cannot be explained as due to epitaxial growth because of the disordered surface of the ITO substrate. It should be remembered that the transport of the chemical species needed for the film growth such as nitrate, Zn^{2+}, and TSPcM is vertical to the two-dimensional plane of the ITO substrate in this electrodeposition process. Consequently, the most efficiently growing (100) crystal face points toward the bulk of the solution to build up the stacking disks. Although the exact structure of the dye layer on ZnO is to be clarified in separate experiments, the chemical interaction between the neighboring disk planes, probably bridging through TSPcM molecules, leads to epitaxial-like alignment of the disks around the *c*-axis within the stacks.

Formation of TSPcZn Assemblies in the ZnO/TSPcZn Films. Although the chemical interactions between the ZnO surface and TSPcM lead to the observed change of the crystal structure of ZnO, a formation of ordered assemblies of the dye molecules on the surface of ZnO is also observed. The electronic interaction within such ordered dye aggregates leads to specific changes of the electronic structure of the dye molecules and thus can nicely be studied by monitoring UV−vis absorption spectra. In Figure 5 are shown the absorption spectra of the ZnO/TSPcZn thin films electrodeposited at −0.7 and −0.9 V, compared with those

(52) Murakoshi, K.; Kano, G.; Wada, Y.; Yanagida, S.; Miyazaki, H.; Matsumoto, M.; Murasawa, S. *J. Electroanal. Chem.* **1995**, *396*, 27.
(53) Falaras, P. *Sol. Energy Mater. Sol. Cells* **1998**, *53*, 163.
(54) Nazeeruddin, M. K.; Kay, A.; Rodicio, I.; Humphry-Baker, R.; Müller, E.; Liska, P.; Vlachopoulos, N.; Grätzel, M. *J. Am. Chem. Soc.* **1993**, *115*, 6382.

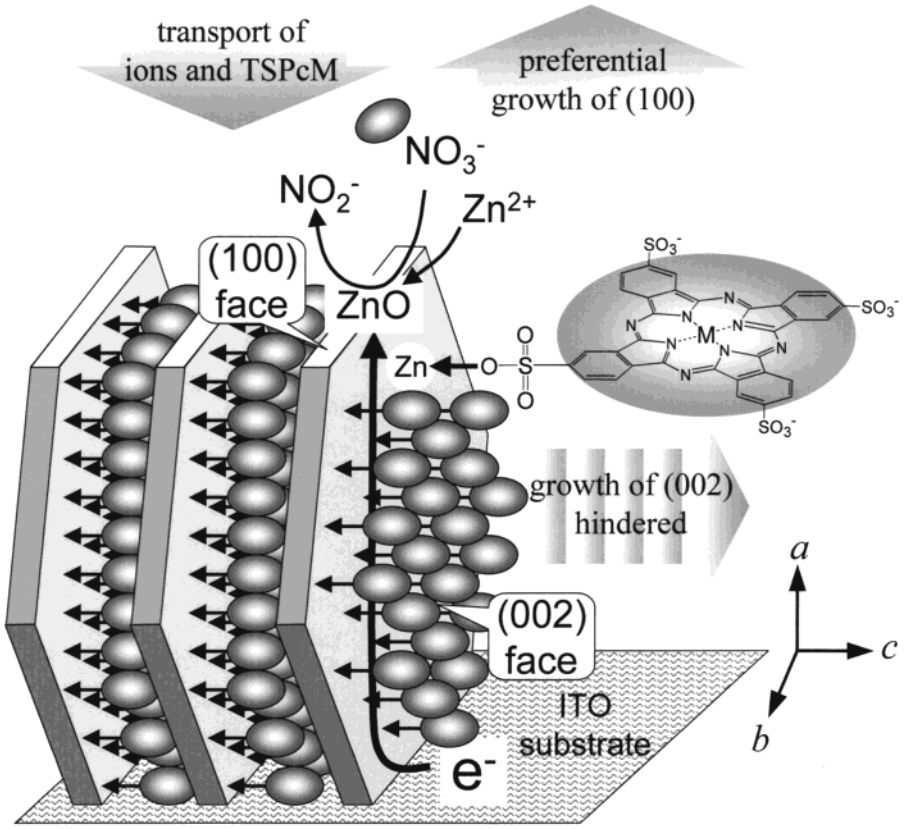

Figure 4. Illustration of the self-assembly of the ZnO/TSPcM thin films by one-step electrodeposition, showing the preferential adsorption of TSPcM onto the (002) planes of ZnO and consequent preferential growth of (100) planes to create the stacking "disks" aligned vertical to the substrate.

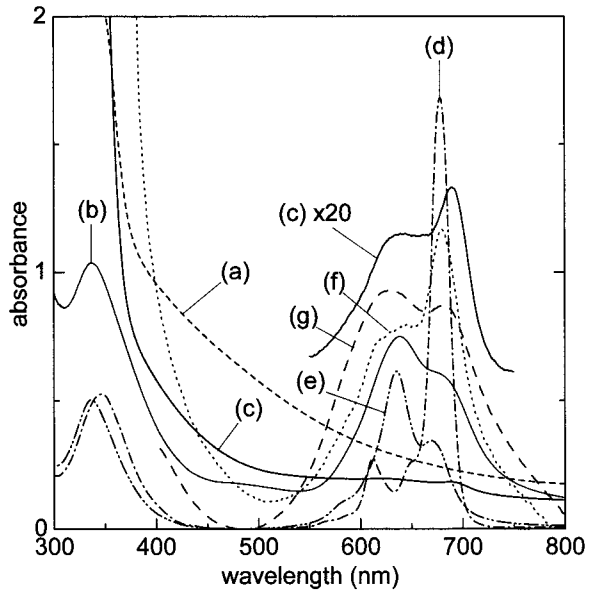

Figure 5. UV−vis absorption spectra of the ZnO thin film electrodeposited at −0.9 V (a), ZnO/TSPcZn thin films electrodeposited at −0.7 (b) and −0.9 V (c), aqueous solutions of TSPcZn in its monomeric form measured in the presence of CTAC (d) and dimeric form without CTAC (e), physical mixture of dry powders of ZnO and TSPcZn (f), and ZnO powder to which TSPcZn is chemically adsorbed from its aqueous solution (g).

of the pure ZnO thin film, an aqueous solution of TSPcZn, an aqueous solution of TSPcZn with added CTAC, a dry mixture of solid TSPcZn and ZnO powders, and ZnO powder to which TSPcZn is adsorbed by refluxing it in an aqueous solution of TSPcZn.

As noted earlier, the electrodeposited ZnO thin film is translucent and milky white. It only exhibits a sharp increase of the absorption below ca. 380 nm attributable to the band gap absorption of ZnO, aside from the apparent gradual increase of absorption with decreasing wavelength because of light scattering (Figure 5a). Both of the ZnO/TSPcZn thin films deposited at −0.7 and −0.9 V were blue and more transparent than the pure ZnO, yet their absorption spectra showed a remarkable difference. The film deposited at −0.7 V was intensely blue, exhibiting absorption maxima at 337 and 639 nm and a shoulder at around 680 nm (Figure 5b), whereas the film deposited at −0.9 V was pale blue and has a Q-band absorption peak at 690 nm and a shoulder at around 630 nm, as clearly seen in the enlarged spectrum (Figure 5c).

The intermolecular attraction due to the strong π-electronic affinity between TSPcZn molecules leads to the formation of dimers in a face-to-face arrangement of the Pc ring system even when dissolved in water.[39] Formation of such assemblies of Pc molecules can be characterized by a clear blueshift of the Q-band absorption peak from that of the monomer, because of the π-electronic interaction in a parallel arrangement of the chromophore.[39,55,56] This π-stacking aggregation of disklike TSPcM molecules can only be suppressed in the presence of a cationic detergent such as CTAC.[39] Ab-

(55) Hunter, C. A.; Sanders, K. M. *J. Am. Chem. Soc.* **1990**, *112*, 5525.

(56) Stillman, M. J.; Nyokong, T. In *Phthalocyanines*; Lezznoff, C. C., Lever, A. B. P., Eds.; VCH: New York, 1989; Vol. 1.

sorption spectra of monomeric TSPcZn are therefore obtained only for a mixed aqueous solution of TSPcZn and CTAC, which exhibits a sharp Q-band absorption peaking at 678 nm and a Soret-band absorption at 347 nm (Figure 5d). The absorption spectrum of dimeric TSPcZn is obtained for an aqueous solution of TSPcZn without CTAC, for which both of the two absorption peaks are blueshifted to 635 and 336 nm, respectively (Figure 5e).

Clear resemblance between the absorption spectra of the ZnO/TSPcZn film deposited at −0.7 V and the dimeric TSPcZn in water indicates formation of π-stacking aggregates for the TSPcZn molecules in the ZnO/TSPcZn film. The aggregates in the film obviously differ from solid TSPcZn that was precipitated in water by adding ethanol (Figure 5f). The dry solid TSPcZn powder was physically mixed with dry ZnO for measuring its absorption spectrum in diffuse reflection. The solid TSPcZn exhibits an absorption peak at 679 nm, close to that of monomeric TSPcZn in water, although the absorption peak is significantly broadened. Such absorption character speaks for an amorphous structure of solid TSPcZn, for which random intermolecular interaction is expected to cause simple broadening of the absorption spectrum. The electrodeposition obviously does not result in the formation of such random aggregates of TSPcZn but does generate ordered aggregates.

Formation of ordered assemblies of TSPcZn on the ZnO surface was further proven by preparing a TSPcZn-modified ZnO powder by refluxing commercial ZnO powder in an aqueous solution of TSPcZn. Its absorption spectrum has a character very similar to the ZnO/TSPcZn film deposited at −0.7 V, exhibiting absorption maxima at 633 and 681 nm (Figure 5g). TSPcZn is adsorbed as π-stacking aggregates on a ZnO surface. Formation of such ordered dye aggregates on inorganic surfaces was reported by Nüesch et al. for merocyanine dyes adsorbed on TiO_2, Al_2O_3, and ZrO_2, as a consequence of chemical interactions between the dye molecules and the ordered surface of inorganic materials as well as that among the neighboring dye molecules.[57] Monolayer adsorption of dye molecules in an ordered structure was also observed directly by AFM for SAM of modified azobenzene dyes on a gold surface.[37]

In our electrodeposition process, TSPcZn molecules not only interact with the surface of ZnO but also among the molecules to promote self-assembly of ordered TSPcZn aggregates while affecting the growth of ZnO crystallites. The spectrum of the ZnO/TSPcZn film deposited at −0.9 V, on the contrary, has a Q-band absorption character similar to the monomer (Figure 5c). It is therefore obvious that TSPcZn exists mainly as a monomer in the film deposited at −0.9 V. The absorption peak of TSPcZn in the film (690 nm) is redshifted from that of monomeric TSPcZn in water (678 nm), suggesting an electronic interaction with ZnO, because of its chemical attachment to the ZnO surface. It should be noted that TSPcZn is dissolved as dimers in the deposition bath, because it does not contain CTAC. In this case, the interaction of TSPcZn with the ZnO surface separates TSPcZn aggregates to incorporate them in monomer form, probably because of the increased pH at the vicinity of the electrode due to the accelerated reduction of nitrate, which should result in a higher solubility of TSPcZn.[39,41]

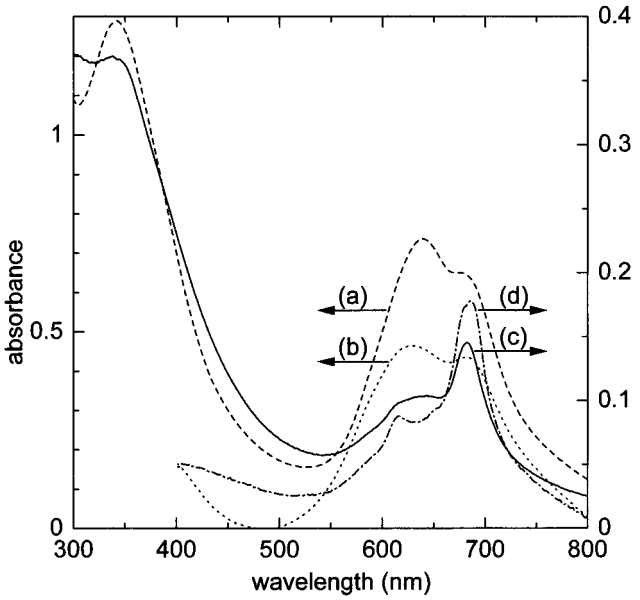

Figure 6. UV−vis absorption spectra of the "as-prepared" ZnO thin film electrodeposited at −0.7 V (a), ZnO powder modified with TSPcZn by reflux treatment (b), and the same samples after removal of the aggregates unbound to ZnO by soaking them in a 0.1 M CTAC aqueous solution (c) and (d), corresponding to (a) and (b), respectively.

Further insights about surface aggregation of TSPcZn were obtained by treating the ZnO/TSPcZn film deposited at −0.7 V and the TSPcZn-modified ZnO powder by an aqueous CTAC solution (Figure 6). TSPcZn produces π-stacking aggregates in both of them, as seen in the spectra before the treatment (Figure 6a,b). Although the dyes could not be removed by rinsing them with pure water, soaking them in an aqueous solution of CTAC immediately turned the color of the solution blue, because of the dissolution of TSPcZn. However, the remaining film and the powder still remained blue, although much less intensely. After the CTAC-treated samples were carefully rinsed with pure water and dried in air, their absorption spectra were again measured (Figure 6c,d). Very interestingly, both of them showed a monomer-like absorption peak in the Q-band region, just like that of the ZnO/TSPcZn film deposited at −0.9 V. It is evident that the CTAC treatment only dissolved surface π-stacking aggregates of TSPcZn and left the surface-bound TSPcZn monomer. The remaining monomeric TSPcZn could only be removed from ZnO by being dipped in alkaline such as 0.1 M KOH. No change was seen when the ZnO/TSPcZn film deposited at −0.9 V was dipped in the CTAC solution, because TSPcZn already exists as a monomer. It should also be noted that the adsorption of TSPcZn did not occur at all when CTAC had already been added to the bath for film deposition or the solution for dye adsorption onto the ZnO powder, suggesting that CTAC blocks the interaction between sulfonic acid groups of TSPcZn and the ZnO surface. It yielded only pure ZnO thin film.

From these experimental findings, the adsorption modes of TSPcZn on ZnO during film deposition at −0.7 and −0.9 V and the effect of the CTAC treatment are

(57) Nüesch, F.; Moser, J. E.; Shklover, V.; Grätzel, M. *J. Am. Chem. Soc.* **1996**, *118*, 5420.

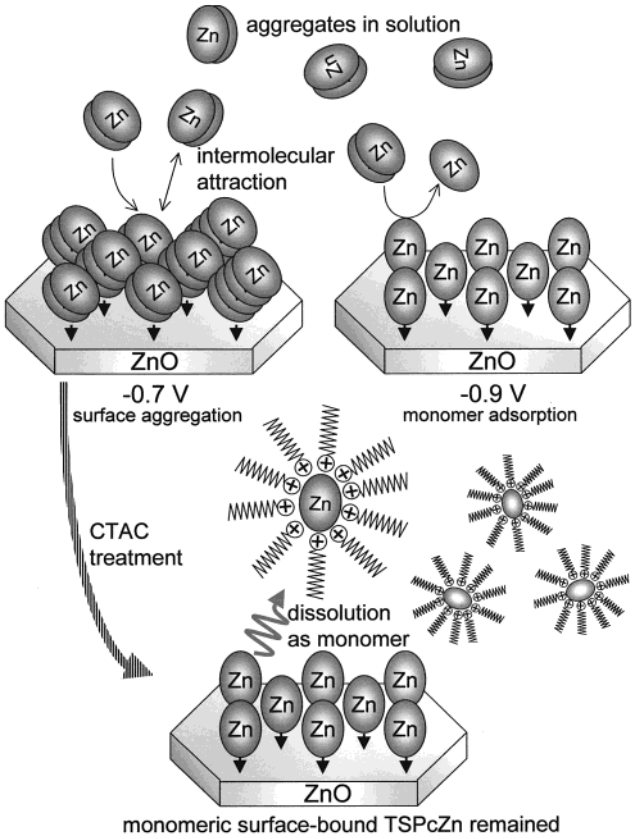

Figure 7. Surface aggregation of TSPcZn because of the intermolecular attraction for the film deposited at −0.7 V and the monomeric adsorption of TSPcZn for the film deposited at −0.9 V because of the relative increase of ZnO growth rate. The treatment of the film deposited at −0.7 V by CTAC aqueous solution dissolves the surface aggregates, leaving only surface-bound monomeric TSPcZn molecules.

summarized as illustrated in Figure 7. At −0.7 V, the intermolecular attraction among TSPcZn molecules establishes π-stacking aggregates of TSPcZn on the ZnO surface, leading to a high concentration of TSPcZn in the film (Table 1). When a larger overpotential was applied (−0.9 V), the dimers of TSPcZn are cleaved upon their adsorption on ZnO to produce a film in which TSPcZn exists as a monomer. The CTAC treatment of the ZnO/TSPcZn film deposited at −0.7 V succeeded in dissolving only π-stacking aggregates on the surface of ZnO and leaving the surface-bound TSPcZn monomer. It is not likely that a part of TSPcZn remained somewhere inaccessible by solvent, such as voids in ZnO crystals, because the same spectral change was seen with the treated ZnO powders for which the dyes could be present only at the surface.

Influence of the Central Metal to TSPcM Assemblies. The aggregation behavior of TSPcAl and TSPcSi was very different from that of TSPcZn as both aqueous solutions and in the electrodeposited films (Figures 8 and 9). π-stacking aggregation of TSPc in water is largely hindered for a complex of trivalent Al(III), because of the presence of axially coordinating anions such as Cl^-[38] or OH^-,[39] although lowering the pH of the solution was found to promote aggregation and adding CTAC suppressed aggregation.[41] The aqueous solution of TSPcAl (without CTAC) exhibits a sharp Q-band absorption peak at 680 nm, clearly indicating

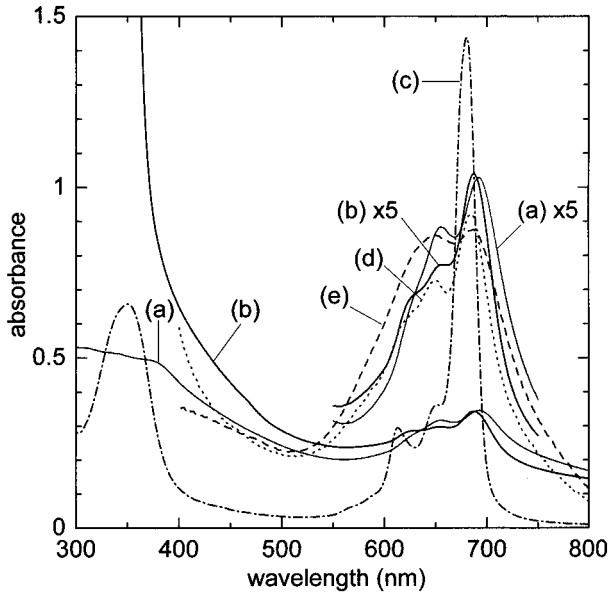

Figure 8. UV−vis absorption spectra of the ZnO/TSPcAl thin films electrodeposited at −0.7 (a) and −0.9 V (b), aqueous solution of TSPcAl (c), physical mixture of dry powders of ZnO and TSPcAl (d), and ZnO powder to which TSPcAl is chemically adsorbed from its aqueous solution (e).

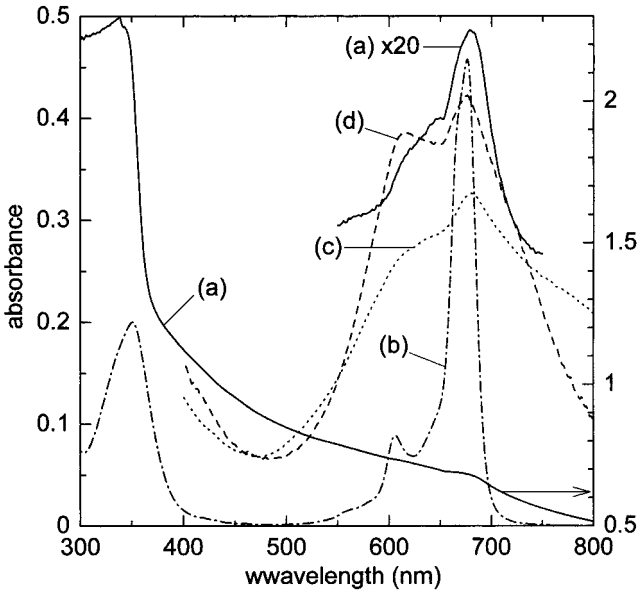

Figure 9. UV−vis absorption spectra of the ZnO/TSPcSi thin film electrodeposited at −0.9 V (a), aqueous solution of TSPcSi (b), physical mixture of dry powders of ZnO and TSPcSi (c), and ZnO powder to which TSPcSi is chemically adsorbed from its aqueous solution (d).

dissolution of TSPcAl as a monomer in neutral (pH = ca. 6) water (Figure 8c). Although solid TSPcAl shows a somewhat broad but monomer-like absorption character in the Q-band region with maxima at 648 and 685 nm, indicating its amorphous structure (Figure 8d), reflux treatment of ZnO powder in an aqueous solution of TSPcAl (as monomer) results in formation of π-stacking aggregates of TSPcAl on the ZnO surface, as characterized by the significant broadening of Q-band absorption toward shorter wavelength, exhibiting maxima at 647 and 687 nm (Figure 8e). It is supposed that TSPcAl molecules are so concentrated when adsorbed on ZnO that they form aggregates because of the

increased intermolecular affinity, even though they tend to aggregate to a much lower extent than TSPcZn. It has been found that TSPcAl resides mainly in its monomer form in each of the ZnO/TSPcAl thin films electrodeposited at −0.7 (Figure 8a) and −0.9 V (Figure 8b), as indicated by a higher absorption in the longer wavelength part of the Q-band. It should be noticed, however, that TSPcAl is slightly aggregated in the film deposited at −0.7 V, as found by the relative increase of the left-hand peak absorbance, compared to the film deposited at −0.9 V. It is likely that the deposition under more negative potential effectively suppresses surface aggregation of TSPcAl, same as the change seen with TSPcZn. Because of the suppressed aggregation of TSPcAl, its concentration in the electrodeposited film was not as high as that in the ZnO/TSPcZn thin film deposited at −0.7 V (Table 1). The effect of the deposition potential on the dye loading was therefore not as significant as that with TSPcZn. The deposition at −0.9 V resulted in approximately half the concentration of TSPcAl in the film (Table 1).

Because TSPcSi has two axial OH^- coordinating to the central tetravalent Si(IV), its π-stacking aggregation is almost completely prohibited.[41] As far as TSPcSi was soluble, aggregation of TSPcSi was not detected by lowering the pH.[41] Addition of CTAC thus had no effect on the aggregation behavior of TSPcSi. The absorption spectrum of aqueous solutions of TSPcSi has all of the features expected for monomeric Pc, with a sharp Q-band absorption peak at 676 nm (Figure 9b). Solid TSPcSi seems to have stronger intermolecular interactions than solid TSPcZn and TSPcAl, because the Q-band absorption is significantly broadened. Adsorption of TSPcSi onto ZnO powder by reflux treatment still allowed π-stacking aggregation of TSPcSi, as indicated by the clear broadening of the Q-band absorption toward shorter wavelengths, creating a peak at 614 nm (Figure 9b). This is probably due to the same reasons as those discussed for TSPcAl. TSPcSi therefore does produce certain ordered aggregates when it is highly concentrated. However, it exists purely as a monomer in the electrodeposited film, as characterized by the clear resemblance of the Q-band absorption peak of the films to that of the monomer (Figure 9a). It is seen that TSPcSi tends to aggregate to the smallest extent among the three compounds tested in this study and that it accounts for its lowest concentration in the deposited films (Table 1).

Conclusion

Cathodic electrodeposition from aqueous mixed solutions containing zinc nitrate and TSPcZn, TSPcAl, or TSPcSi has been found to realize self-assembled growth of ZnO thin films whose surface is modified by these dyes. The addition of the dye molecules changed the morphology of the ZnO films drastically. A very unique "stacking disk" structure was found for the ZnO/TSPcSi film. XRD analysis of the deposited films have revealed that the adsorption of the dye molecules switched the orientation of ZnO crystallites by 90°, from the (002) parallel with substrate arrangement to the (100) parallel with substrate arrangement. TEM observation of the deposits coupled with electron beam diffraction analysis clarified the fine structure of the stacking disks, in which the edge and the disk plane correspond to (100) and (002) crystal faces, respectively. It was also found that the disks are perfectly aligned with respect the *c*-axis within the disk stack. A growth model was presented in an attempt to explain the reasons for the evolution of the disklike crystals with the observed arrangements, where the adsorption of TSPcM is supposed to take place preferentially onto the (002) planes of ZnO, considerably attenuating the further crystallization of ZnO on these planes so that the crystal tends to grow along the (100) direction.

The self-assembly during the electrodeposition process appeared not only as the influence of dye adsorption to the ZnO crystal growth but also as formation of ordered dye aggregates on the ZnO surface. Because TSPcZn produces π-stacking aggregates in the deposition bath due to the intermolecular attraction, TSPcZn is adsorbed as a multilayer of π-stacking structure in the film deposited at −0.7 V, causing a characteristic blueshift of the Q-band absorption. Aggregates of the same quality were also found for TSPcZn-modified ZnO powder samples. These surface aggregates were completely removed by dipping them in a solution of CTAC and leaving only surface-bound monomeric TSPcZn. Film deposition at more negative potentials (−0.9 V) suppressed the aggregation of the dye, yielding a ZnO/TSPcZn film in which TSPcZn exists mainly as a monomer, although the smaller aggregation resulted in a lower surface concentration of TSPcZn. The aggregation in solution is hindered for the complexes of trivalent Al^{3+} and tetravalent Si^{4+} because of the presence of axially coordinated OH^-. Although their adsorption to ZnO powders by reflux treatment brought about their aggregation on the ZnO surface, the electrodeposition yielded thin films in which monomeric dyes are predominant.

It has been found that the evolution of these novel inorganic/organic mixed materials is purely a self-assembly, depending upon a subtle balance of the chemical interaction of ions and molecules with the growing ZnO surface and the chemical interaction among those ions and molecules themselves. It should be emphasized that these materials having ordered structures at atomic and molecular levels were obtained without consuming any notable energy, unlike the gas-phase processing of the materials. These new materials with the structures specially chosen by the constituents themselves are expected to possess new properties. The difference in the formation of the dye aggregates is especially interesting in view of their ability as photosensitizers.[34] Work is currently in progress for the elucidation of the photoelectrochemical properties of these self-assembled ZnO/TSPcM thin films.

Acknowledgment. The authors are grateful to G. Schneider (University of Bremen) for preparation of the TSPcM dyes and for discussions of their optical properties in solution, as well as to D. Lincot (CNRS-Paris) for fruitful discussions. The present work is partly defrayed by the Grant-in-Aid for Scientific Research on Priority-Area-Research "Electrochemistry of Ordered Interfaces" from the Ministry of Education, Science, Sports and Culture of Japan (09237105). Financial support by DFG (Schl 340/ 3-1,3) is gratefully acknowledged.

CM980619O